ISAS - INTERNATIONAL SCHOOL FOR ADVANCED STUDIES

International School for Advanced Studies
Trieste

The effect of repeated stimulation of the optic nerve on evoked field potentials in the frog optic tectum

Thesis submitted for the degree of
"Magister Philosophiae"

CANDIDATE
Marco Atzori

SUPERVISOR
Prof. Andrea Nistri

Academic Year 1992/93

TRIESTE

SISSA - SCUOLA INTERNAZIONALE SUPERIORE DI STUDI AVANZATI
TRIESTE
Strada Costiera 11

International School for Advanced Studies
Trieste

The effect of repeated stimulation of the optic nerve on evoked field potentials in the frog optic tectum

Thesis submitted for the degree of
"Magister Philosophiae"

CANDIDATE
Marco Atzori

SUPERVISOR
Prof. Andrea Nistri

Academic Year 1992/93

Notes

Part of this thesis has been submitted for publication:

Non-monotonic decay of excitatory synaptic transmission in the frog optic tectum following repetitive stimulation of the optic nerve *in vitro*

M. Atzori and A. Nistri

and congress communication:

1. An unusual feature in the fatigue-dependent processes at the frog optic tectum

   M. Atzori and A. Nistri

   17th Gif Lecture in Neurobiology
   Mechanism and Regulation of Neurotransmitter Release
   December 3-4 1992

2. The effect of repeated stimulation of the optic nerve on the evoked field potential in the frog optic tectum.

   M. Atzori and A. Nistri

   Physiological Society Meeting
   Southampton
   September 27-29 1993

Contents

Chapter 1

The role of the optic tectum in the frog visual system

1.1 Introduction

This study is dedicated to understanding some features of the visual system of the frog. Like for the majority of lower vertebrates, the frog visual system has a moderate resemblance with mammals one, having respectevely fewer cortical centers for the analysis of visual information. In spite of its simpler structure, only some gross features underlying visual signal processing in frog are well uderstood, while the details both at the cellular level and at the circuit level still have to be investigated. The aim of our work was, as it will be pointed out forward, to use a relatively simple technique such as that of extracellular field potential recording, to detect effects related to the presence of a local inhibitory network whose existence has been revealed by a variety of electrophysiologic and non-electrophysiologic methods.

1.2 Generalities of the visual system in vertebrates

The two pathways of the visual signal for lower vertebrates and for mammals, shown in the scheme of fig.1.1, are essentially the same.

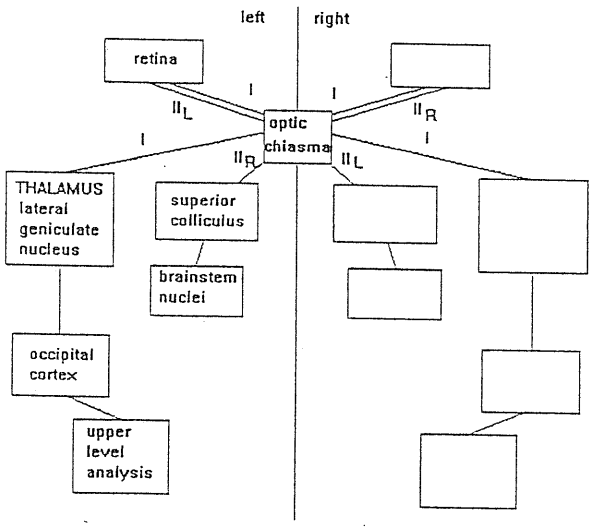

Fig.1.1 Schematic representation of the visual system in vertebrates:
Two anatomically and functionally distinct pathways constitute the main output from the retina. Path I is more developed in higher vertebrates while II is the main visual path in lower vertebrates. From the OT a further descending path returns back to the retina.

From the retina the component I, is split in the optic chiasma into ipsilateral and contralateral visual fields, and sent to the lateral geniculate nuclei (LGN) of the contralateral and ipsilateral thalamus respectively. Hence the projections are sent further on to the occipital cortex and than to the upper level centers along the visual pathway. On the other hand, the component II is fully crossed at the level of the optic chiasma projecting monosynaptically to the contralateral superior colliculus (SC), that is the anatomical structure phylogenetically correspondent to the optic tectum (OT) of lower vertebrates. A major output from OT or SC is sent down to the brainstem nuclei. The main difference between lower and higher vertebrates concerning their visual system is the relative importance of each one of the two pathways: in the former the retino-tectal path represents the 80-90% of the optic ganglion fibers while the rest is the retino-thalamo-cortical tract, in the latter the proportions are nearly inverted. This is not surprising if we look at the development of telencephalon in lower and in higher vertebrates, but it is not the only known difference. In fact in the majority of higher vertebrates, ganglion cells display relatively simple receptive field properties whereas higher level properties of the visual signal such as movement are processed forward along the visual pathway.

1.3 Role of the Superior Colliculus

The fact that the retino-tectal projection in lower vertebrates is substantially mantained in higher vertebrates in spite of the huge increase of the extratectal retinic afferents is suggestive of an important role played by this structure, a role that seems not to be overwhelmed even by the more refined but necessarily slower processing of the highly polysynaptic processing in the striate and extrastriate cortices.
A first recognized task of the OT/SC is multimodal sensory integration. In fact although the OT/SC main input is from the optic nerve also acustic, tactile and in the case of certain snake species infrared eye (Mkrtycheva,1964; Kobayashi et al., 1992) inputs have been recognized in the OT/SC of the majority of the investigated species. For each type of input there is in the OT/SC a topographical representation of the environment surrounding the animal's head. In particular for the visual input, it is known since the studies of Gaze (Gaze,1958; Jacobson,1962) that dorsal retinal quadrant projects to the posterolateral OT, nasal quadrant to the posteromedial, the ventral quadrant to the anteromedial and the temporal quadrant to the anterolateral.
Another fundamental finding is that in all studied species, ranging from salamander to primates, a focal electrical stimulation in the OT/SC induces a well defined "saccade", a movement bringing a particular point of the visual field to the center of the animal's retina (Manteuffel and Roth,1993; Hepp et al.,1993; Glimcher and Sparks,1993,Munoz and Wurtz,1992). This movement is generally achieved with a rapid eye movement, but in many species it is accompanied with or even substituted by a small neck or body movement like in salamanders or in owls. It is generally believed that the movements associated with the saccade are generated sending a command from the OT/SC to the brainstem nuclei, which act as a time integrator for the afferent signal (Bosch and

Paul,1993). In the brainstem nuclei the information coding for the direction of the saccade should be transformed into the pattern (relative proportion) and strength for the activation of the suitable motoneurones. In primates the SC is one of the centers which coordinates the motor input of the brainstem with signals sent by several areas: from parietal and frontal cortex as well from ventral tegmental area of the basal nuclei as shown in fig.1.2 .

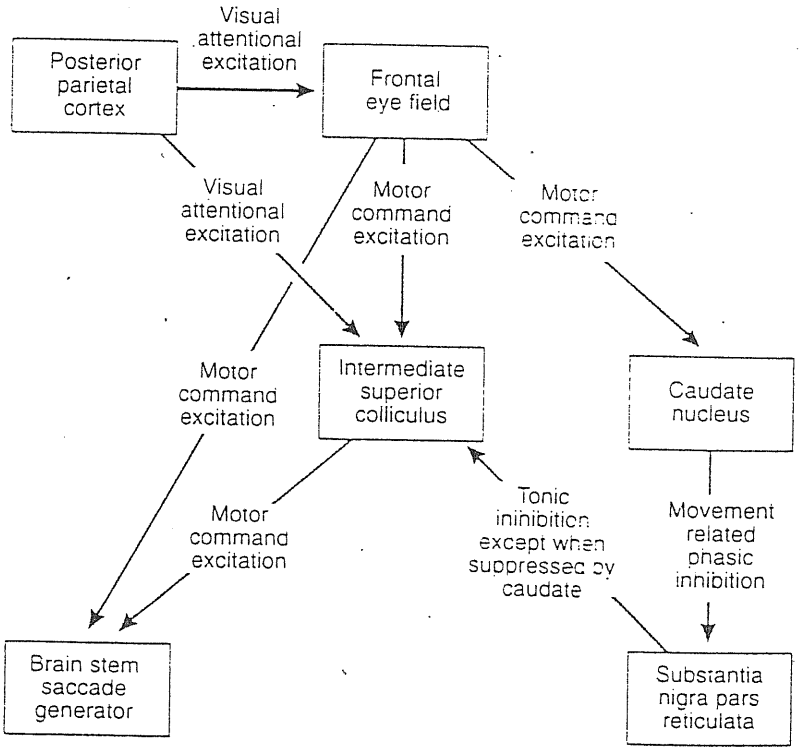

Fig. 1.2 Higher control of saccadic eye movements.
The SC receives direct excitatory projections from the frontal eye field and from the posterior parietal cortex, and an inhibitory projection from the substantia nigra pars reticolata. Nigral inhibition can be suppressed by the caudate nucleus, which in turn receives a motor command from the frontal eye field (from Kandel, Schwartz, Jessel).

1.4 Anatomy of the frog optic tectum.

The OT in the frog consists of two simmetric lobes surrounding the lateral ventricoles, limited caudally by the small sized cerebellum and rostrally by the isthmus separating it from the telencephalon. Instead of the six layers wrapping the higher vertebrate largest amount of cortex surface, the OT displays in frog as well as in all of lower vertebrates a 9-layered structure, substituted by a 7-layer one in mammals. The outer layer receives the retinic afferents and is further subdivided into seven sublayers. The precise distribution of the layers slightly differs between species. Afferent and efferent connections to and from frog OT are schematically shown in the schemes of fig.1.3 A,B (Lazar,1984).
On morphologic basis Lazar recognizes several types of intrinsic neurons having different distributions within the OT layers: large and small pyriform cells, whose cell bodies are distributed mainly in layers 2,4,6 and in layer 6 respectively, fusiform cells, oriented either perpendicularly or parallel to the OT surface, with cell bodies mainly in layer 8 and 9, and stellate and amacrine cells mainly in layer 9. The majority of OT efferent neurons are either pyramidal cells with 160-250 μm dendritic arborization and cell bodies in layer 6 or ganglionic cells with dendritic arborization up to 1 mm wide. Hystochemical studies showed the presence of the nicotinic acetylcholine receptor (Sargent et al.,1989), of the glutamate receptor (McDonald et al.,1989) as well as of a very strong GABAergic system (Antal et al.,1991) in nearly all species of studied frogs. These findings have been confirmed by electrophysiologic measures (Sivilotti and Nistri,1988; Sivilotti and Nistri, 1988; Sivilotti and Nistri 1989;Nistri et al.,1990). The effect of the presence of such a large GABAergic system should presumably in principle affect not only the single cell level but also the extracellular multi-unit signal evoked by some pattern of optic nerve stimulation.

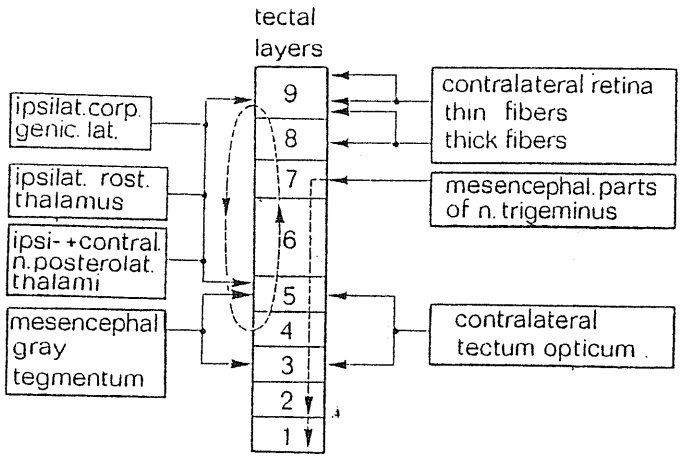

Fig.1.3 Afferent connections of the Optic Tectum.
From Lazár (in Vanegas, 1984).

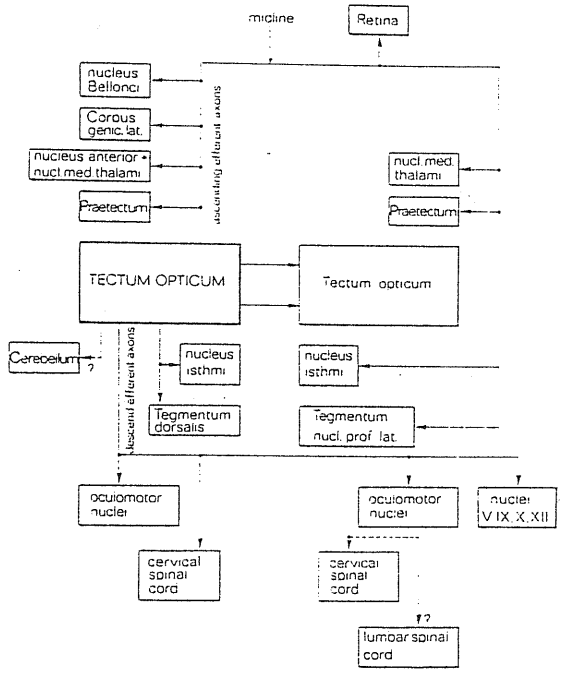

Fig.1.4 Efferent connections of the Optic Tectum
From Lazár (in Vanegas, 1984).

1.5 The visual system of the frog

It is known since the work of Maturana and co-workers (Maturana et al., 1968) that ganglion cells of the frog optic nerve carry nearly exclusively signals produced by objects moving across their visual field. In the work of Maturana and co-workers the response to real visual stimuli were recorded extracellularly with tungsten electrodes in the optic nerve as well as in the OT, from single cells. To report the words of Maturana and collegues: "... the ganglion cells form five natural classes, four of which perform on the visual image complex analytical operation which remain invariant under the most varied environmental conditions, while the fifth measures the light intensity." The five classes of ganglion cells are :
class 1: sustained edge detection
class 2: convex edge detection
class 3: changing contrast detection
class 4: dimming detection
class 5: dark detection .
Maturana and collegues have also evaluated the velocity of conduction for class 1-4 cells:"The operation for classes 1 and 2 are performed by small ganglion cells with unmyeliniated axons that conduct at speed of 0.5 m/s or below. The operations for classes 3 and 4 are performed by cells with myelinated axons conducting at speeds from 1 to 8 m/s, the fastest being the one of the fourth class."

Chapter 2

Field potentials in the frog OT

2.1 Theory of the field potentials

The field potential is defined as the extracellular potential coming from the ensemble of neurons surrounding the electrode. The field potential is the weighted sum of the components coming from each and every of the surrounding cells, in which the weights for every component are a complex function of the distance of the neighbour current vector and of their intensity and directions. The field potentials produced by a group of cells reflect in an indirect way the membrane potential changes, namely the synaptic and action potentials which the cells undergo in unison. A study of such potentials is therefore an important prerequisite for the understanding of the characteristics of any neural assembly. When the anatomical arrangement of a neural assembly is known, the activity of a pool can often be treated as if generated by a small number of elements, each one representing the average behaviour of the particular set of cells activated synchronously from specific sites. Well-known examples of field potentials are the electro-cardiogram (ECG), the electromyogram from the cardiac muscle, and the electro-encefalogram (EEG), the field potential recorded from the scalp. The cellular element underlying the field potential generation is described in fig.2.1 (from Hubbard, Llinàs and Quastel, 1969, modified).

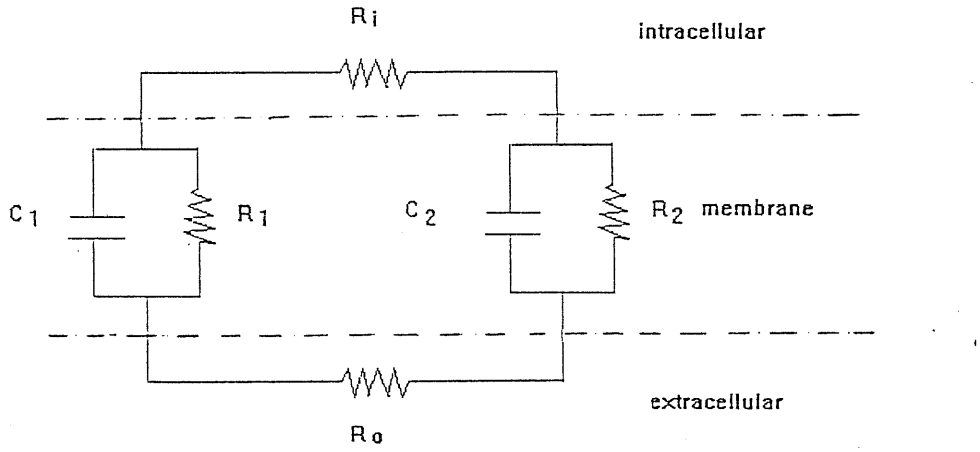

Fig.2.1 Sink and source of the electrical activity of a nerve cell.
The cell is regarded as a circuit with a low resistance part (extra- and intra-cellular) and a higher resistance part in the membrane. The latter is further subdivided into dendritic tree (C_1,R_1) and cell body (C_2,R_2). A current flowing from the extracellular to the intracellular environment at the left side of the circuit induces a current of opposite sign in the right part (see text).

The equivalent circuit for a cell is given by three compartments: intracellular, extracellular and membrane. The first and the second are regarded as a homogeneous, low resistance *milieu* whereas the latter has dishomogeneous and substantially higher resistance. Stimulation triggers the presynaptic release of neurotransmitter in the synaptic cleft. The neurotransmitter induces a large increase in the postsynaptic conductance that, in turn, generates a dendritic current and a subsequent variation of the local electrical potential, having an opposite sign in respect to the inward current. As a first approximation, the lowest resistance sites of the active nerve cell are the soma and the dendritic tree. We can apply Kirchoff's law to the closed circuit in fig.2.1.: if a large corrent flows into the cell at the dendritic level the same amount of current with opposite sign must subsequently cross the circuit. Sites in which positive or negative current flows into cells are called respectively "sinks" and "sources". In a layer-structured tissue, using this simplified cell model, the sinks and sources correspond then to the dendritic and somatic layers respectively.

2.2 Field potentials in the frog OT

An analysis of the field potentials in the frog OT has been done by Chung et al. (1974). In this work an analysis was applied to the laminar structure of the tectum, aimed at the localization of the sinks and sources. Optic nerve stimulation yields four waves with different time course and a certain degree of temporal overlapping. According with the sink-source analysis their relative proportion depends on the depth of the recording electrode. Following the nomenclature of Maturana and collegues the two waves with the shortest delays from stimulation, coming from myelinated fibers, are named m_1 and m_2, while the latest, from unmyelinated boundles, are named u_1 and u_2. The m_1 wave has been detected only in a single preparation by Chung and co-workers, presumably because of its quite short latency from the stimulus artifact. The correspondence between the classes of cells recorded *in vivo* and the field potentials *in vitro*, should be
u_1 wave: sustained edge detection
u_2 wave: convex edge detection
m_1 wave: dimming detection
m_2 wave: changing contrast detection .
A complete correspondence between the cellular classes found by Maturana and co-workers *in vivo* and the extracellular waves detected *in vitro* seems to exist, considering also that the fifth class of *in vivo* cells is quite rare and spread along the tectal layers.

2.3 Preparation and solutions

Frogs of the species Rana Temporaria were kept at room temperature in suitable humidity environment and with light/dark cycles of 24 hours. They were anaesthetized with immersion for some minutes in a 0.1% solution of tricaine methanesulfonate just before being decapitated. The brain was removed in Ringer solution under ice opening

the skull from above after setting the optic nerve free using a transpalatal approach. The composition of the Ringer solution was (mM) NaCl 111, KCl 2.5, $NaHCO_3$ 17, NaH_2PO_4 0.1, $CaCl_2$ 2.5 and glucose 4. The osmolarity was 234 mOsm. During some experiments a "Low Ca^{2+}" solution was used consisting of 1.75 mM $CaCl_2$ plus 0.75 mM $MgCl_2$. Picrotoxin (75 µM) was used to block chloride-mediated inhibitory processes (Sivilotti and Nistri 1991). The solution was oxygenated with a mixture of 95% O_2 and 5% CO_2 (pH=7.3). The bath temperature was kept between 9°C and 10°C with the help of a close-circuit cooler.

2.4 Experimental setup

The apparatus for stimulation and field potentials recording is shown in fig.2.1 .

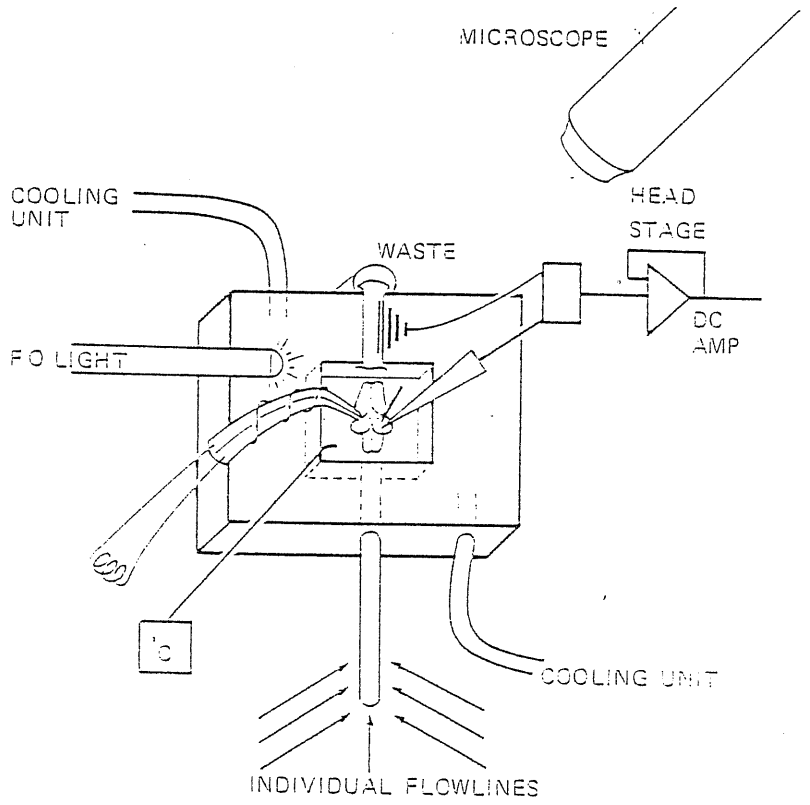

Fig.2.2: Recording chamber for frog whole brain.
The brain is immersed in the chamber superfused with the oxygenated Ringer solution. The chamber contains an inbuilt water jacket through which the cooling liquid circulates. The temperature of the Ringer was 9-10°C. The suction electrode tightly takes up a few millimeters of the optic nerve contralateral to the measuring electrode. Visual control is achieved with a 40X microscope illuminated by an optic fiber.

One millisecond-long stimulations were applied to the contralateral optic nerve through a low resistence suction electrode. The recording electrode, filled with 3 M NaCl, had a resistence of 2-10 MΩ and was placed at a depth of 100 μm from the outer surface of the OT. Evoked EPSPs (0.3-3.0 mV) were amplified with an Axoclamp 2A unit and further 200-fold amplified before being digitized at 4 KHz by a Labmaster interface connected to an IBM-PC computer (fig.2.2).
Both acquisition and signal analysis were performed using the pCLAMP software (version 5.5) in the pulse mode.

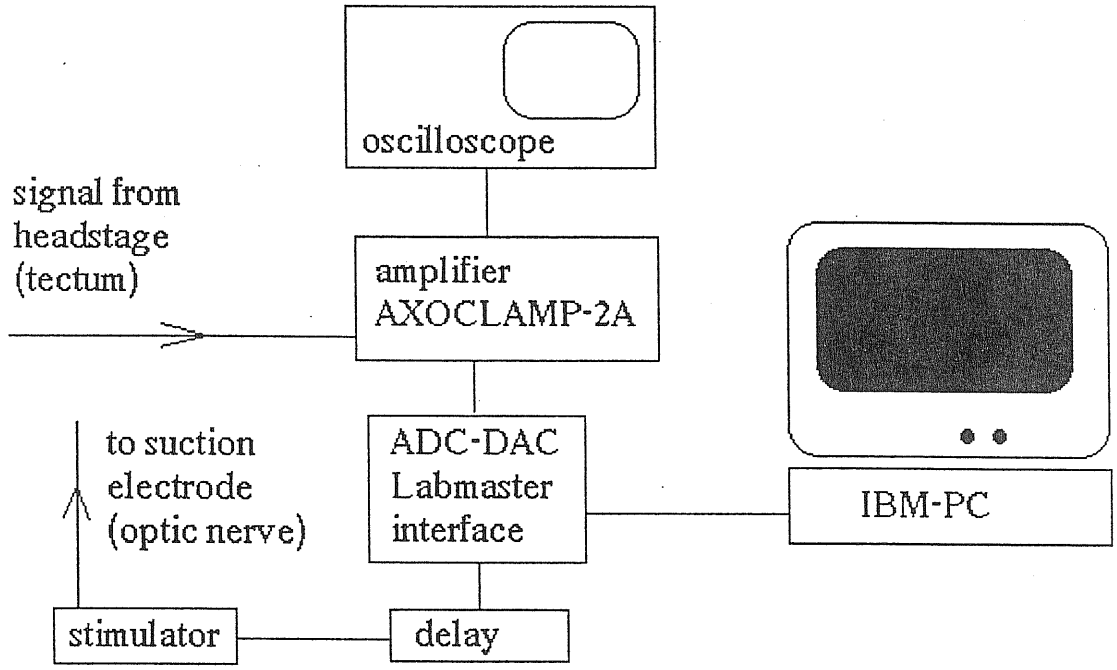

Fig. 2.3: Recording system.
The signal coming from the OT was send to an amplifier that reduces the impedence of the input signal. At this point the signal can be digitized by an ADC board and stored in a PC mass memory.

Chapter 3

Changes of synaptic efficacy in the frog OT due to repeated stimulations

3.1 Methods

Thirty one adult frogs of both sexes were used for the experiments. The preparation was superfused in the recording chamber with the Ringer solution at a rate of 5-8 ml/min. Depending on the depth of the recording electrode, the m_2, u_1 and u_2 waves were identified as those having latencies of 9.9±1.0 ms, 41.9±2.5 ms and more than 120 ms respectively from the stimulus artifact (fig.3.1 a-c).

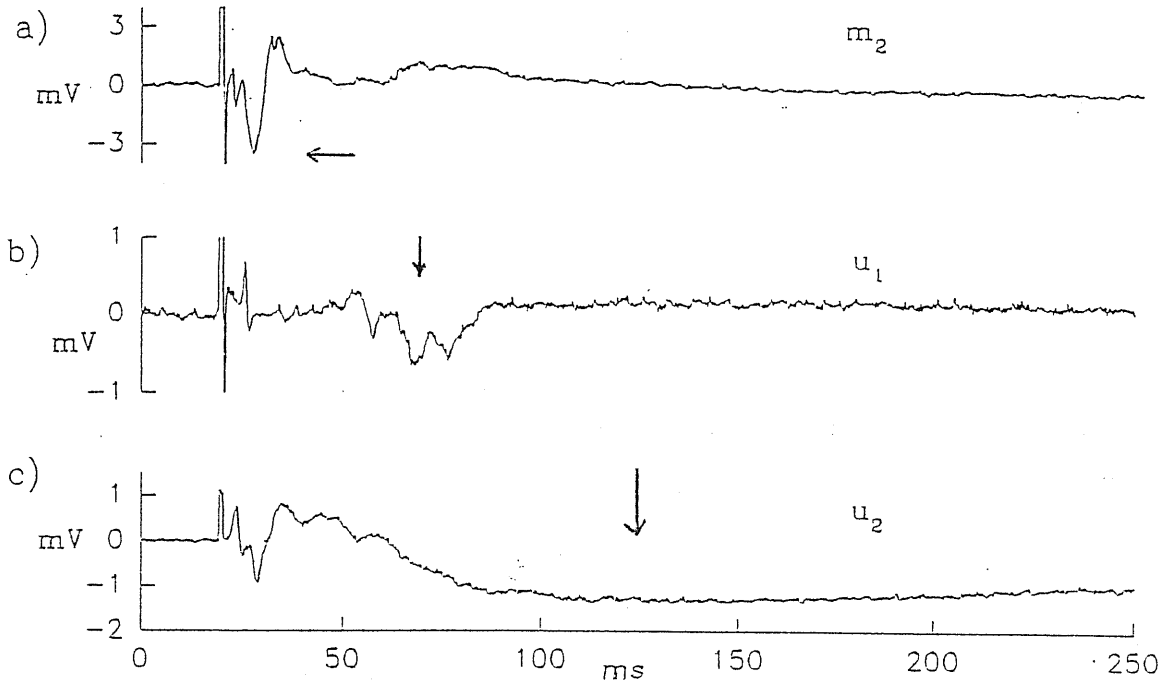

Fig. 3.1. Synaptic field potentials recorded from the frog OT in control solution. a,b,c: representative recordings of the m_2, u_1 and u_2 respectively from three different preparations stimulated at 0.033 Hz.

While all preparations displayed reliably recorded m_2 and u_1 waves, the u_2 wave was detected less frequently under the present experimental conditions of recording depth and stimulus strength (Chung et al. 1974). The reproducibility of measurements was tested at the beginning of each experiment by stimulating at very low frequencies (0.033 Hz) which consistently induced stable waveforms. A minimum of 60 s was consequently chosen as a safe interval to obtain recovery from any modifications produced by higher frequency pulses. Input/output curves were used for determing the stimulation threshold and the minimum stimulation intensity to induce a maximal response for each wave. Maximal stimulations were usually in the 10-40 V range that is at least 10 times larger than the threshold value for stimulation, although intensities up to 65 V were occasionally applied. Submaximal stimulations were defined as those eliciting 50-70% of the maximal response. Preparations showing reliable responses for at least 3 hours were used, although the average survival of the preparations was much longer.
Because of a possible overlap of the waves in some region but not in the peak region, the peak amplitude of the m_2 and u_1 responses and the response of the u_2 at 150 ms from the stimulus artifact were measured rather than their integrals. The data are given as means ± s.e.m. . Statistical analysis of related samples was done using the Student's *t*-test for the differences for numerical values and the Wilcoxon test for the differences in ranked measures (Colquhoun 1971). Only differences with $p < 0.05$ were accepted as significant.

3.2 Trains of pulses at low frequency

Trains of 5 to 20 pulses at various frequencies (0.1-1.0 Hz) were applied to evoke responses which were averaged (n=4). While in 8 preparations a monotonic decay of synaptic transmission following train stimulation appeared, for the majority of preparations (23/31) the amplitude of the synaptic responses declined during the stimulus train in a non-monotonic fashion since the first few responses after the first one were reduced in respect to the later ones before a steady state amplitude was eventually reached (fig.3.1 d). The amplitude of this phenomenon was often directly related to the stimulation frequency as shown in fig.3.2.

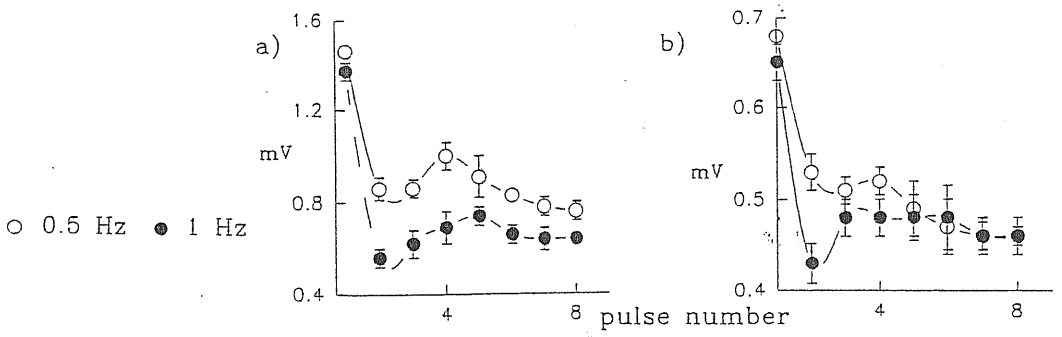

Fig. 3.2: Development of synaptic fatigue at different stimulation frequencies in control saline solution. a,b: pattern of synaptic fatigue at different frequencies (0.5 or 1.0 Hz) for the m_2 and the u_1 waves, respectively (n=4). A spline fits the data.

For a quantitative estimate of the non-monotonic decay of synaptic transmission a simple parameter was calculated, namely the variation from the linear decay (VLD). VLD was defined as the difference between the interpolated value of the smallest response (assuming linear decay from the first one to the next largest response) and the observed amplitude of the same response:

$$VLD = \frac{T-E}{A} x 100 \; ; \; T = m(x_{min} - x_A) + A \; ; \; m = \frac{B-A}{x_B - x_A} \qquad \text{eq.(1)}$$

this is exemplified in fig.3.3:

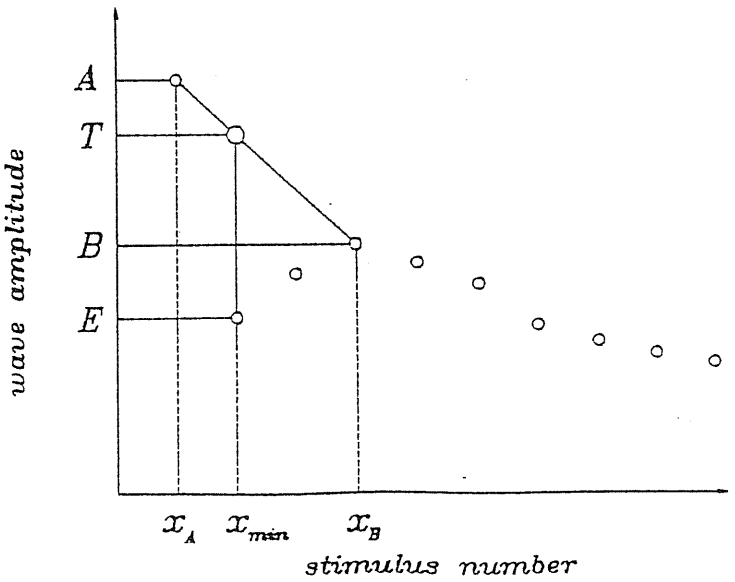

Fig.3.3: schematic diagram to show method to calculate VLD during the early part of the synaptic fatigue (see text); the small circles represent the experimentally-observed points, the large circle is the linearly interpolated value of the smallest response.

At 0.1 Hz the VLD values for all three waves were rather small (≤ 10%) or even negative in the case of the m_2 waveform (fig. 8). Raising the stimulation frequency to 1 Hz gave significant VLD increases for the three responses whereas intermediate frequencies (0.33 or 0.5 Hz) produced significant VLD values only for the u_1 response (fig.3.4) .
Since at 1 Hz stimulation rate all the waves displayed the non-monotonic decay pattern (with full recovery after 60 s rest), experiments were carried out at this frequency to explore whether a local network might have been involved in synaptic fatigue. A polysynaptic system may be expected to require a certain stimulation threshold for its activation: the intensity of the stimuli was therefore reduced with consequent decrement in postsynaptic response amplitude.

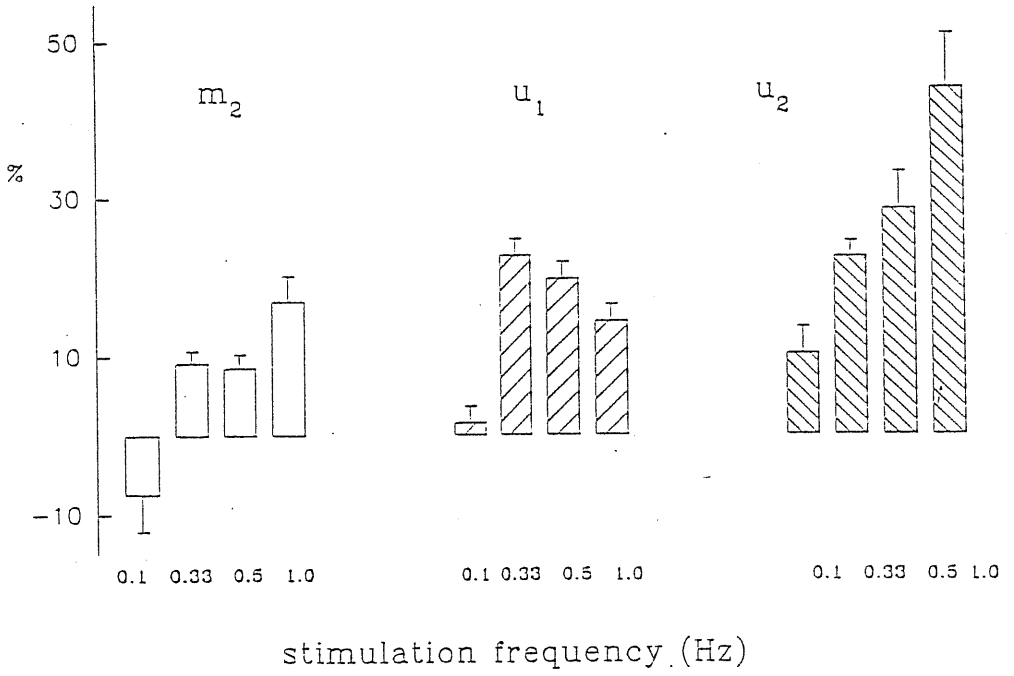

Fig.3.4: Histograms of VLD changes for various stimulus frequencies shown at the bottom of each bar, generating the m_2 (left), u_1 (middle) and u_2 (right) synaptic waveforms (n=7).

Fig.3.5 demonstrates that weaker stimuli also elicited less fatigue and smaller variations in the early part of the decay pattern, while the amplitude of the afferent volley elicited by strong pulses was found essentially unchanged for frequencies up to 1 Hz .

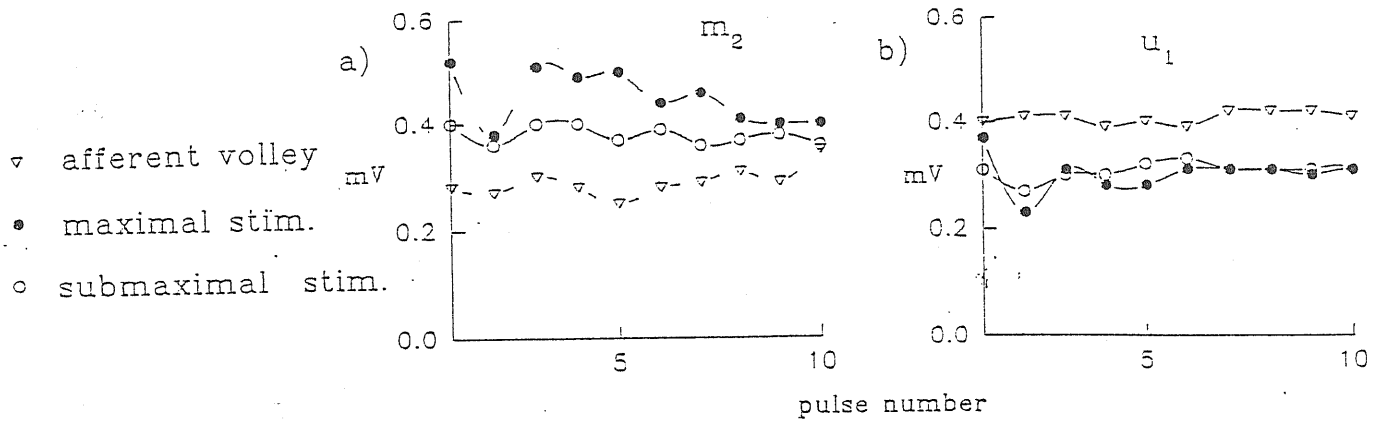

Fig.3.5: Representative examples of differential sensitivity of the synaptic fatigue process to changes in stimulation intensity. a,b: plot of changes in amplitude of the m_2 and u_1 waves vs. pulse number in a train following strong or weak stimuli always applied at 1 Hz. The amplitude of the afferent volley ( ) recorded during the same experiment is also shown. Note that changes in amplitude are absent for the afferent volley, slight for the field potentials elicited by weak stimuli and much larger for the field potentials evoked by strong stimuli. The data were fitted by a spline curve.

Since the work of Dodge and Rahamimoff (1967) it is known that the amount of neurotransmitter released at the frog neuromuscular junction is a linear function of the third to fourth power of the concentration of external calcium ($[Ca^{2+}]_o$) (for a review see Erulkar, 1983). Even if it is unknown whether a similar relation applies to frog central synapses, the activation of an interneuronal pathway would be expected to add responses which are more critically dependent on $[Ca^{2+}]_o$ than monosynaptic transmission. A reduction in $[Ca^{2+}]_o$ from 2.5 to 1.75 mM should therefore induce not only a decrease in the EPSP amplitude but also a comparatively much larger fall in the influence of any polysynaptic pathway. This phenomenon was in fact observed as shown in fig.3.6.

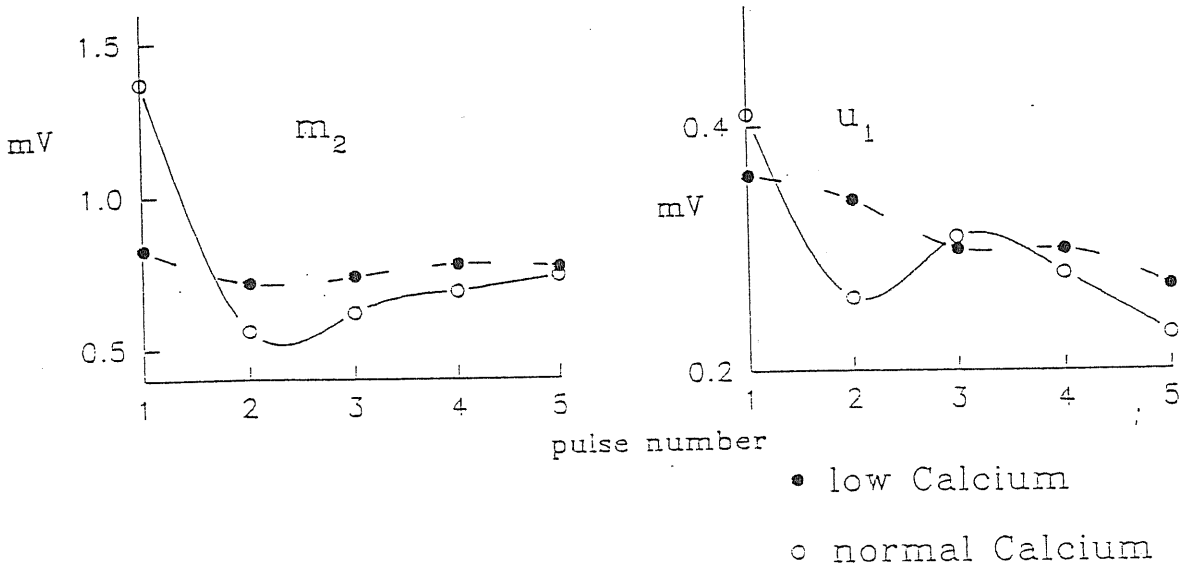

Fig.3.6 : differential sensitivity of the synaptic fatigue process to $[Ca^{2+}]_o$. a,b: plot of changes in amplitude of the m_2 and u_1 waves vs. pulse number in a train following strong or weak stimuli always applied at 1 Hz. Data were fitted by a spline curve. Reduction and smoothing of the synaptic fatigue process produced by strong stimuli at 1 Hz in a low $[Ca^{2+}]_o$ solution (o) for the m_2 (a) and u_1 (b) waves when compared with similar data recorded from the same preparation in control saline (o).

A polysynaptic inhibitory pathway would possibly utilize GABA, a major neurotransmitter in the frog brain (Sivilotti and Nistri 1991), for this purpose. In order to block GABA receptor systems completely picrotoxin (75 μM) was added to the Ringer solution. In separate experiments this picrotoxin concentration was found to be the largest one just subthreshold for induction of convulsive activity. After 10-15 min exposure to picrotoxin all three waves were significantly reduced : the m_2 decreased by 0.54±0.17 mV, the u_1 by 0.62±0.15 mV and the u_2 by 0.32±0.11 mV (n=10). When tests for synaptic fatigue were performed, it was shown (fig. 3.7) that in picrotoxin solution this phenomenon for the m_2 and the u_1 waves was less dramatic than in control, and lacked transient recovery. These results are thus comparable to those obtained with low $[Ca^{2+}]_o$ or with submaximal stimulations. Table 1 reports the differences between the VLD values during treatment and in control conditions for the same preparation .

test for m_2	arithmetic average	geometric average	p<	n
Low Ca^{2+}	13.4 ± 3.5	12.0 ± 3.8	0.05	7
submaximal stimulus	12.3 ± 3.8	11.1 ± 4.1	0.05	7
picrotoxin	13.0 ± 1.4	12.7 ± 1.7	0.05	7

test for u_1	arithmetic average	geometric average	p<	n
Low Ca^{2+}	13.4 ± 4.2	12.5 ± 4.7	0.05	6
submaximal stimulation	20.1 ± 6.0	17.2 ± 6.4	0.05	6
picrotoxin	24.9 ± 2.3	23.7 ± 3.4	0.05	6

test for u_2	arithmetic average	geometric average	p<	n
Low Ca^{2+}	31.6 ± 9.5	28.1 ± 10.7	0.05	6
submaximal stimulus	18.1 ± 4.1	14.8 ± 4.6	0.05	6

Table 1: change in VLD values during test treatments
Results are expressed as the difference between VLD data in control solution and those during one of the treatments listed in the first column. Values are aritmethic and geometric averages ± s.e.m. with n = number of experiments. P values were obtained with the Wilcoxon test on related samples (Colquhoun, 1971). Data for the u_2 wave in picrotoxin solution are not included as they were recorded from only two preparations.

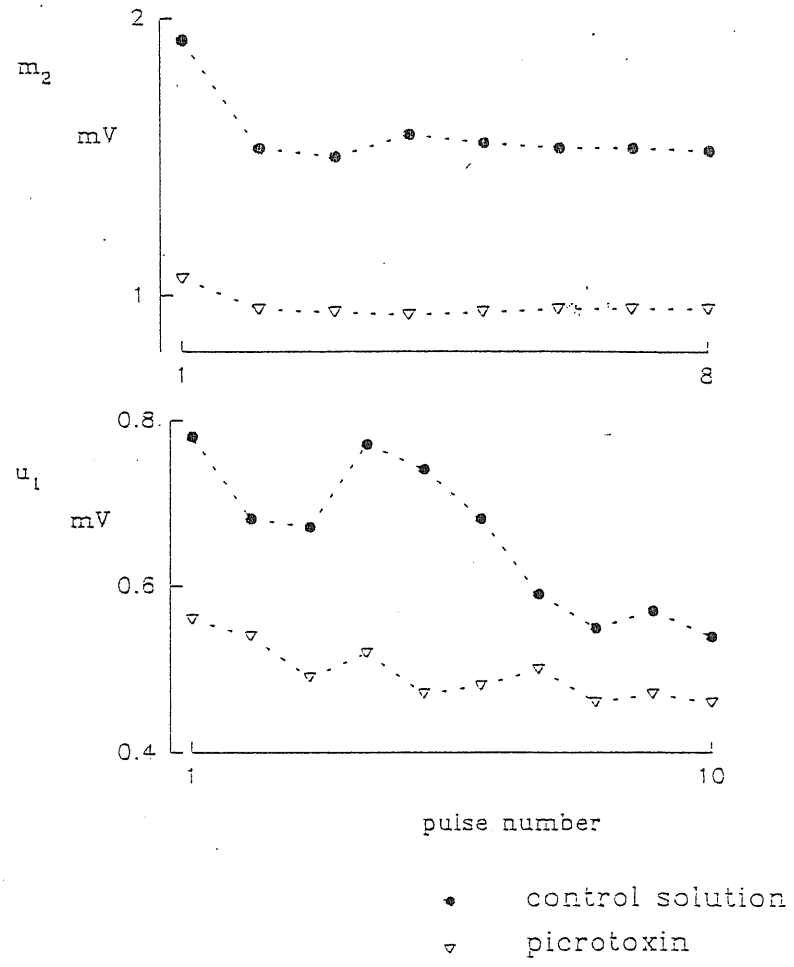

Fig.3.7: Effect of 75 μM picrotoxin on synaptic fatigue pattern. Top and bottom diagrams are from a representative experiment showing the time course of m_2 and u_1 waveforms (produced by strong stimuli at 1 Hz), respectively. Picrotoxin was added to control saline after recording drug free responses ( ). Datapoints (joined by straight lines) in picrotoxin solution ( ) were obtained after 20-30 minutes exposure to this agent.

3.3 Influence of facilitation

In order to test whether short-term changes of neurotransmitter release affected the early dip in the trains of responses, it was of interest to explore the influence of presynaptic facilitation (Magleby, 1987). In the frog OT *in vivo* paired pulse stimulation of the optic nerve at intervals < 1s induces facilitation for all three synaptic waves (Chung et al. 1974). This finding reflects a general property of chemical synaptic transmission, perhaps caused by enhanced presynaptic Ca^{2+} channel activity (Ikeda 1990). In the present experiments the amount of facilitation was quite large, as shown by the example of fig.3.8 .

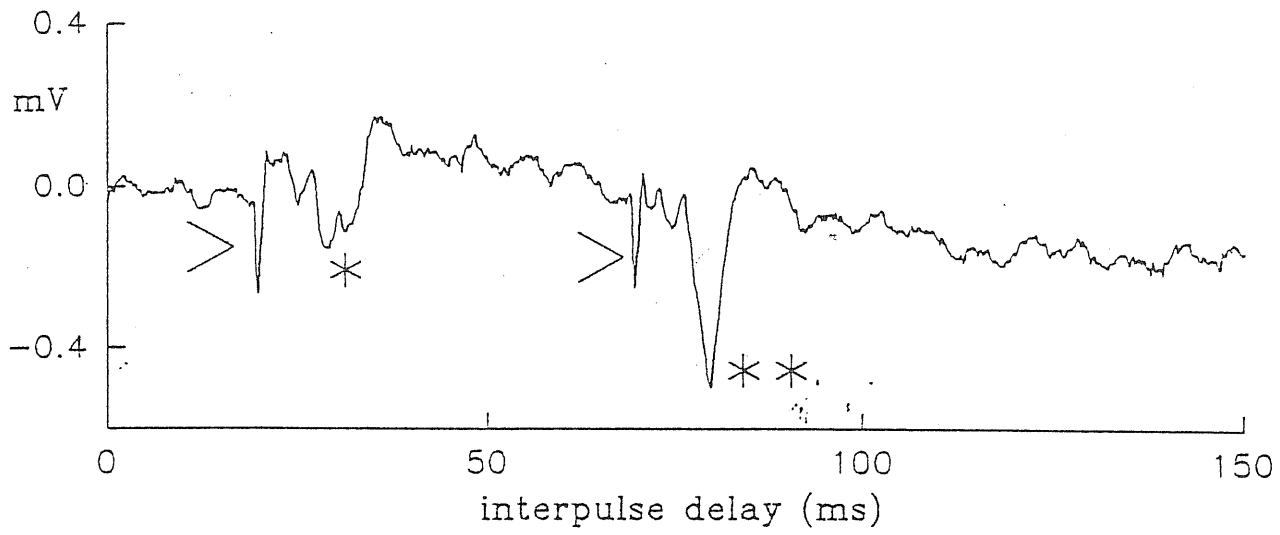

Fig.3.8 . Paired pulse facilitation of excitatory transmission in the frog OT. a: example of facilitation of the m_2 wave; compare response produced by 50 ms interpulse delay (**) with the one (*) obtained without prepulse; arrows show the stimulus artifact.

To avoid problems caused by the overlapping of different waves elicited by pulse pairs, a control trace with only the first response was digitized, and then a second trace with the two consecutive responses was obtained for each interpulse interval. Subtracting the first trace from the second one gave the amplitude of the facilitated response, which was normalized by dividing it by the first control response. Graphs showing facilitation as a function of the interpulse interval are reported in fig. 3.9. Both maximal and submaximal responses were found to be facilitated for pulses closer than 300-400 ms, but a different behaviour occured at interpulse delays longer than 500 ms (fig.3.9) since submaximal responses showed neither facilitation nor depression while maximal responses replaced their facilitation with depression.

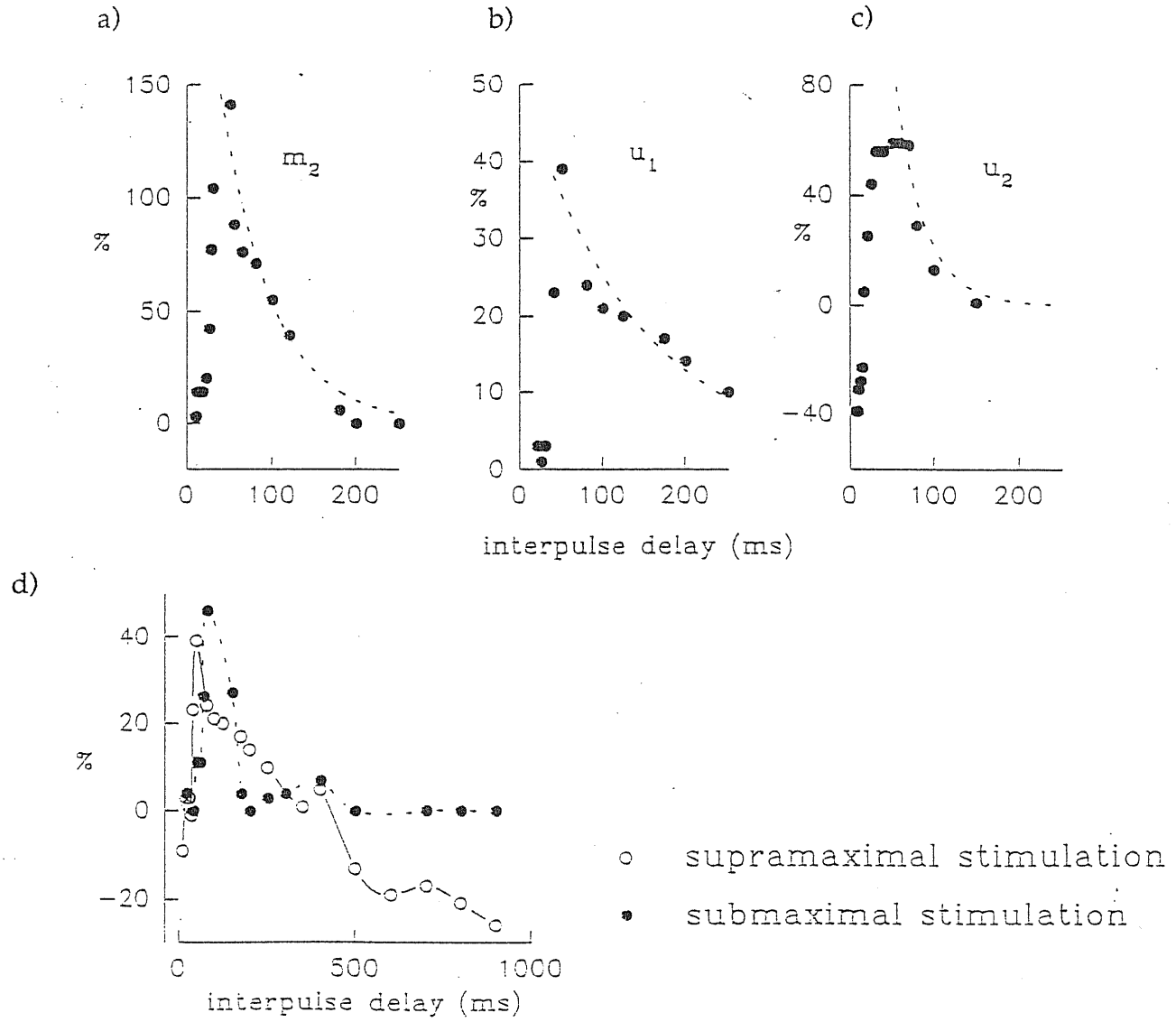

Fig.3.9: Paired pulse facilitation of excitatory transmission in the frog OT. a,b,c: facilitation of m_2, u_1 and u_2, respectively. Quantitative data for this phenomenon are reported in Tab.2. Dashed lines represent the best fit exponential for facilitation (see eq.4) while filled circles indicate experimental data. Intervals between pulses were chosen to be approximately 5-10 ms up to 100 ms intervals and 20-100 ms for larger intervals (up to 900 ms). Experimental points at smaller intervals than the one producing maximal facilitation were not used for the fitting. d: spline curve plot of % facilitation of u_1 wave by strong (o) or weak (o) pulses vs. interpulse delay. Note that after 500 ms synaptic depression occurred with strong pulses. All data were recorded in control saline.

Facilitation was defined as

$$F = A_2/A_1 - 1 \qquad \text{eq.(2),}$$

(Magleby 1987), where A_1 and A_2 are the amplitudes of the same wave elicited by a single or double pulse, respectively. To evaluate its time course, the following expression (Magleby 1987) was used:

$$\frac{dF}{dt} = J(t)f - rF \qquad \text{eq.(3)}$$

in which J(t) is the delta function corresponding to the pulses, f is the amount of facilitation per pulse and $r=1/\tau$ is the rate constant for the removal of F. Other processes such as augmentation, potentiation or depression (Magleby,197) have not been included. Solution of eq.(3) for paired pulses is

$$F = f\, e^{-t/\tau} \qquad \text{eq.(4)}$$

were t is the interval between pulses.
Using eq.(4) to fit experimental data of fig.3.9 (see dashed lines) showed that facilitation peaked at < 100 ms and was very small after 500 ms. Table 2 provides numerical values obtained for the fitting. Although the limited accuracy of the field potential analysis does not allow to resolve various components of the signal enhancement process, the present results confirm that it was essentially correct to use a stimulation frequency up to 1 Hz for studying synaptic fatigue apparently uncontaminated by facilitation.

	m_2	u_1	u_2
$T_{max\ exper}$ (ms)	38 ± 15	74 ± 41	50
$\%_{max\ exper}$	120 ± 59	52 ± 18	59
f (%)	304 ± 165	59 ± 26	492
τ (ms)	49 ± 19	131 ± 61	35

Tab. 2: paired pulse facilitation values
$T_{max\ exper}$ are the intervals giving the maximal facilitation observed experimentally;
$\%_{max\ exper}$ indicates the experimental maximum facilitation of each waveform expressed as percentage of the first control response.
The parameters f and τ have the meaning given in the text (eq. 4). n=4 for m_2 and u_1 and n=1 for u_2.

3.4 Conclusions from the experimental results

The principal finding of the present study was that fatigue of the excitatory monosynaptic transmission from optic nerve fibres to tectal neurones displayed a complex time course since a strong reduction in the amplitude of the early responses in a train was followed by a temporary recovery and then a final decline to a steady level. This pattern was not an invariable phenomenon since experimental manipulations such as lowering the stimulus intensity, reducing $[Ca^{2+}]_o$ or adding the $GABA_A$ receptor antagonist picrotoxin transformed such a complex phenomenon into a smooth decay of synaptic transmission to a steady plateau.
While the isolated frog OT offered particularly advantageous conditions in terms of histological organization and experimental reliability, it should be noted that electrophysiological responses were recorded with extracellular electrodes located in a multisynaptic network. Nevertheless, the small size of tectal neurones makes rather difficult to record from them with intracellular electrodes (Antal et al., 1986;Sivilotti and Nistri, 1992). Presumably further studies using patch clamp recording should help to minimize this drawback, although the remote axodendritic location of optic nerve excitatory synapses (Chung et al. 1974, Antal et al. 1991) may pose some problems for a precise analysis of synaptic mechanisms. The presently used technique allows to investigate with minimally invasive recording, temporal changes in optic nerve-evoked synaptic activity recorded as monosynaptic, albeit integrated, responses in the OT since this preparation has been extensively employed for studies of visual signal processing which yielded a valuable model of neural network, namely *Rana computatrix* (Arbib 1982). The present data seem thus more relevant to understand the function of the synaptic circuits rather than the molecular processes underlying them.
At low frequencies of optic nerve stimulation there was no decrement in excitatory transmission, but at 1 Hz rate, there was a sharp, early decline, particularly evident when strong presynaptic stimuli were used. These observations suggest that the early dip in synaptic transmission was not caused by lack of synchrony in the activation of presynaptic fibers or temporal failure of the afferent volley (which remained unchanged). The frequency and intensity dependence of the "dip" phenomenon suggested the possible involvement of a local inhibitory mechanism. This view was confirmed by the smoother development of fatigue when extracellular Ca^{2+} was lowered and Mg^{2+} was raised (a smaller concentration of Ca^{2+} could not be used without strong block of synaptic transmission). A clue to the possible identity of the inhibitory system was provided by the block of the "dip" in transmission by picrotoxin, an antagonist of $GABA_A$ receptor mediated responses (Sivilotti and Nistri,1991). While the abundance of GABAergic fibres in the frog OT is consistent with this hypothesis, a role for other inhibitory mechanisms, for instance via $GABA_B$ receptors as found in guineapig neocortical cells (Deisz and Prince, 1989), is not excluded and will require further investigation.
It is generally accepted that paired pulse facilitation is a general feature of chemical synaptic transmission (Katz and Miledi, 1968). In the frog OT a prepulse facilitated the

response to a test pulse when the interval was 20-200 ms (this observation applied both to weak and strong pulses). Nevertheless, when the interval extended beyond 500 ms, facilitation was replaced by depression for responses induced by strong pulses, or by little change in amplitude following weak stimuli. These results confirm the presence of paired pulse facilitation in this preparation and indicate that such a phenomenon did not interfere with synaptic fatigue which was present over a longer time span.

Chapter 4

A semiquantitative model describes fatigue

4.1 Theory of the model

In order to provide a simple description of synaptic fatigue observed following 1 Hz stimulation, a model was used in which only two factors were assumed to control the development of this process. The first one was the depletion of a presynaptic Immediately Available Store (IAS) of neurotransmitter (Llinàs et al. 1981) refilled from a Long Term Store (LTS) of infinite capacity following a first order kinetic. The second factor was a component induced by the onset of an inhibitory process activated by the preceeding excitatory signal and proportional to it. The onset of inhibition was presumed to be much faster than its decay.
Using these assumptions a set of equations was employed to fit the time course of synaptic signals elicited during a train of stimuli. Fig. 4.1 shows results of this type of fitting and provided some parameters relevant for the description of the theoretical model. As indicated in table 3, these were τ_{NT}, i.e. the time constant for refilling of IAS by LTS, α, i.e. a dimensionless constant proportional to the amount of inhibition elicited by each stimulus, and τ_{inh}, i.e. the time constant of the decay of the inhibitory process evoked by each stimulus.
Assuming that synaptic fatigue was produced by a combination of the slow refilling of presynaptic stores simultaneously with the onset of local inhibition, the following iterative equation was used to describe the time course of synaptic fatigue:

$$A_n = kc_n - \alpha I_n \qquad \text{eq.(4.1)}$$

were A_n, the amplitude of the n^{th} waveform normalized to the first supramaximal response, is the difference of two terms, the first one accounting for the repletion of IAS from LTS, and the second one representing the inhibitory process. k (proportional to the amplitude of the first response) is the constant fraction of neurotransmitter concentration released by each pulse, and α ($0 \leq \alpha \leq 1$) is a constant which accounts for the total amount of inhibition. c_n is the (variable) neurotransmitter concentration in the IAS just before the n^{th} stimulation and is given by:

$$c_n = c_{n-1} + (c_0 - c_{n-1})\left(1 - e^{-\frac{\delta t}{\tau_{NT}}}\right) \qquad \text{eq.(4.2)}$$

where c_0 is the asymptotic value for the neurotransmitter concentration in the IAS, τ_{NT} is the time constant for refilling IAS from LTS, and δt is the interpulse delay.
I_n is the fraction of inhibition acting on the n^{th} response and is given by the following expression

$$I_n = I_{n-1} e^{-\frac{\delta t}{\tau_{inh}}} + A_{n-1}(1 - I_{n-1}) e^{-\frac{\delta t}{\tau_{inh}}} \qquad \text{eq.(4.3)}$$

where τ_{inh} is the time constant for intrinsic decay (supposed to be exponential) of the inhibitory neurotransmission. In eq.(4.3) the first term corresponds to the cumulative inhibition present immediately before the n^{th} pulse whereas the second term is the inhibition brought about by the n^{th} stimulus itself. Each time the IAS neurotransmitter concentration is suddenly depleted by a pulse, its refilling from the LTS follows a first order kinetic given by the value of c_n from eq.(4.2).
The initial condition for the iterative equation is given by:

$$I_0 = 0 \, , \, A_0 = 0$$

corresponding to absence of inhibition at the first response.

4.2 Results

Experimental data were fitted with a linear least square routine implemented with a Pascal program. The goodness of the fit was evaluated with the Chi-Square test. All calculations were performed with an IBM-PC 486-based. It is reported the flow chart of the program.
Table 3A gives the mean ± s.e.m. of 3 fittings obtained from four averaged responses of 3 preparations. A Chi-square test with n-5 degrees of freedom (n is the total number of points and 5 is the number of the fitting parameters plus the normalization condition) gave values accettable within at least a 5% confidence level. For the least-square minimization procedure the two trains of responses at maximal and submaximal

stimulation were simultaneously used. Tab.3(B,C) reports the results obtained by fitting the same data separately for supramaximal and submaximal stimulations, respectively. A good agreement was found for all parameters except α for the u_1 wave and τ_{NT} for the u_2 wave.

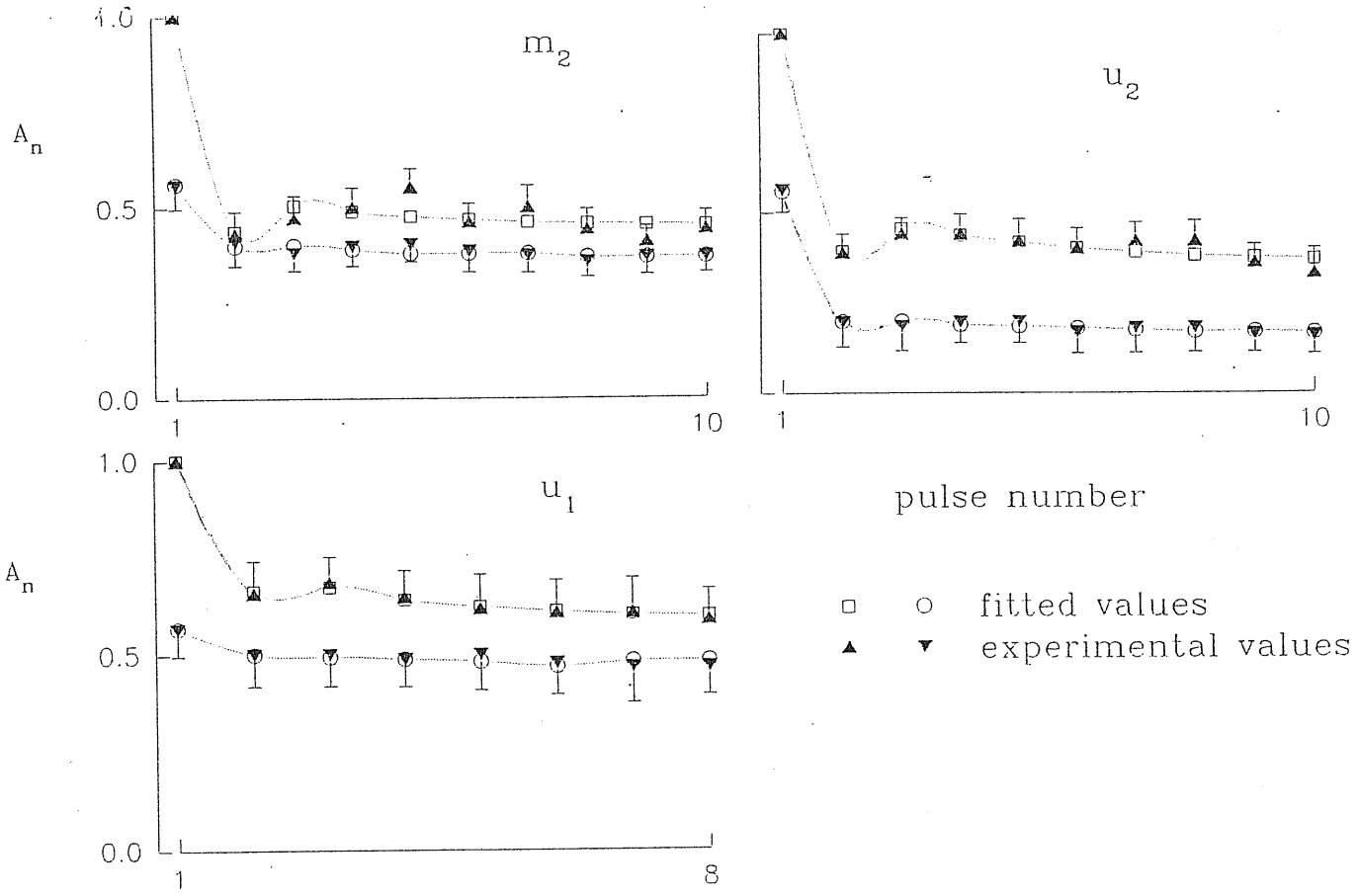

Fig.4.1: Plot of experimental (▲,▼) and simulated (o, □) fatigue process for m_2, u_1 and u_2 waves. Theoretical fitting of datapoints was provided by eq.(4.1-3). Note close correlation between experimental data and computer simulation of fatigue process. Abscissa: number of pulses in the 1 Hz train; ordinate: amplitude of each response (A_n) normalized to the first one elicited by supramaximal stimulation. In each panel the top graph represents responses evoked by supramaximal stimuli while the bottom one shows responses induced by weak pulses (n=4). The parameters derived from the best fitting were for the m_2: τ_{NT} = 4.0 s, α = 0.94, τ_{inh} = 0.77 s,for the u_1 τ_{NT} = 3.1 s, α = 0.78, τ_{inh} = 0.52 s, for the u_2 τ_{NT} = 10.5 s, α = 0.88, τ_{inh} = 2.1 s.

A

	τ_{NT} s	α	τ_{inh} s	R
m_2	3.6 ± 1.7	0.70 ± 0.20	1.1 ± 0.6	0.051
u_1	2.9 ± 0.8	0.74 ± 0.13	0.8 ± 0.4	0.035
u_2	8.8 ± 2.2	0.89 ± 0.05	2.0 ± 0.2	0.032

B

	τ_{NT} s	α	τ_{inh} s	R
m_2	3.7 ± 1.1	0.78 ± 0.17	0.90 ± 0.35	0.034
u_1	4.0 ± 0.5	0.94 ± 0.05	0.79 ± 0.20	0.029
u_2	8.4 ± 2.1	0.90 ± 0.06	3.34 ± 0.90	0.027

C

	τ_{NT} s	α	τ_{inh} s	R
m_2	3.4 ± 1.0	0.67 ± 0.10	0.72 ± 0.28	0.039
u_1	2.6 ± 0.8	0.18 ± 0.04	0.76 ± 0.27	0.033
u_2	4.2 ± 0.8	0.81 ± 0.10	2.3 ± 0.5	0.030

Tab. 3: Parameters obtained from the best fit of the experimental data.
Mean ± s.e.m. of the parameters obtained from the best fit from 3 preparations for each Of the waves. The residuals are expressed as : $R = \sqrt{\{\Sigma_{k=1,N}[A_{exper}(k)-A_{theor}(k)]^2/N\}}$ where $A_{exper}(k)$ and $A_{theor}(k)$ are experimental and calculated normalized values respectively (see fig. 6 legend) with N = number of points. τ_{NT} is the time constant for neurotransmitter transfer from the LTS to the IAS, α ($0 \leq \alpha \leq 1$) is proportional to the inhibition elicited by each stimulation, τ_{inh} is the time constant for the decay of inhibition.
A: values from simultaneous fit for supramaximal and submaximal stimulations; B,C: values from separate fit for supramaximal and submaximal stimulations respectively.

Applying the data of Table 3 to the present model indicates that:
1) refilling IAS from LTS is virtually completed in about 9-12 s for the m_2 and u_1 waves and about 25-30 s for the u_2 wave, which are intervals 3 to 4-fold longer than the respective τ_{NT} values;
2) the values of α derived from the best fitting are near unity, showing that inhibition may provide an important contribution to fatigue of synaptic transmission;
3) the mean value of τ_{inh} is about 1-2 s for all waves, suggesting the involvement of a process faster than neurotransmitter store depletion as the mechanism responsible for the observed depression of early responses.

4.3 A discussion of the model

The model combines a term accounting for synaptic fatigue as slow refilling of a presynaptic store of excitatory neurotransmitter with a term for an inhibitory process (supposed to be similar to lateral inhibition observed in the *Lymulus* eye; Hartline and Ratliff 1972). Presumably, the lag between emptying an immediately available store and its refilling from a long term store underlies the monotonic reduction in the amplitude of excitatory responses to a steady level, which is determined by the rate of transmitter transfer between the two stores. Using these assumptions, experimentally derived parameters were found to produce a good fit of the observed pattern of fatigue. In spite

of the closeness between observed and fitted results, other more complicated models might have been used: for instance, one which introduced a threshold value at which the inhibitory process became operative and/or which contained a factor related to intrinsic fatigue of the inhibitory system.
Computations based on these additional (albeit realistic) assumptions would have required the introduction of at least two other adjustable parameters, with the consequent danger to deal with an *ad hoc* model. The simplicity of the present model in predicting rather accurately the development of synaptic fatigue is an obvious advantage although it cannot entirely explain the observed data. For example, the existence of a threshold for the activation of inhibition, which was left out from the present model, might account for the discrepancy between α values for supramaximal and submaximal stimulations eliciting the u_1 wave. The difference between τ_{NT} after supramaximal or submaximal stimulation might also indicate an additional mechanism causing more severe fatigue elicited by the stronger stimuli. Furthermore, while the model suggests a role for an inhibitory synaptic circuit in shaping fatigue of excitatory transmission, it does not allow a distinction to be made between various types of inhibition, for instance feed-forward and feed-back or pre- and post- synaptic (fig. 4.2). The present data thus highlight the influence which a local inhibitory network can have on sensory inputs and should prompt further work aimed at clarifying the cellular mechanism(s) involved.

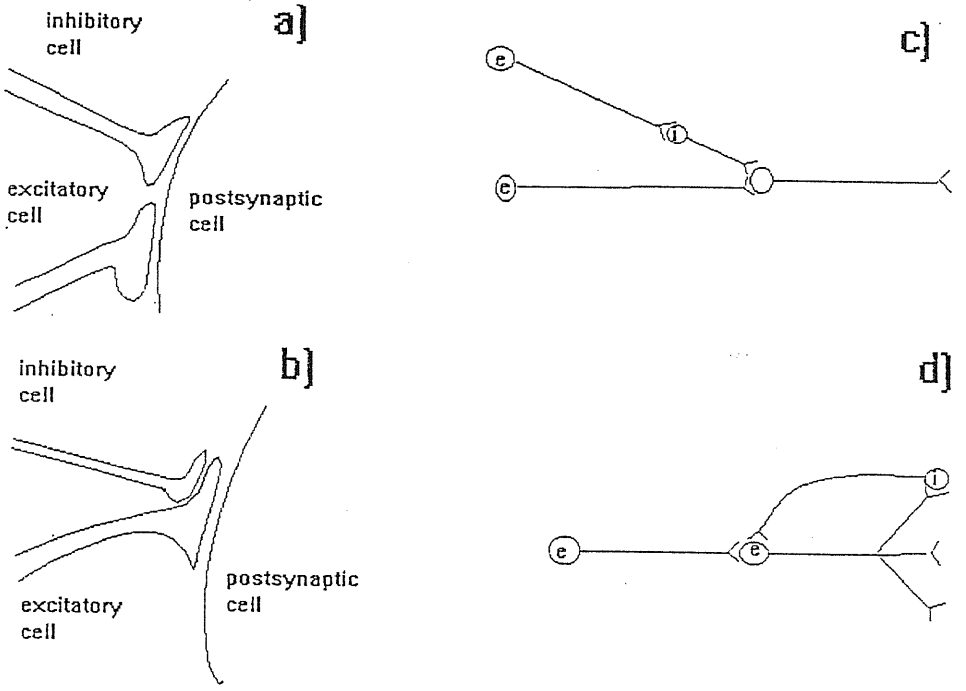

Fig. 4.2: Possible ways in which an interneuronal circuitry can affect the local processing of the afferent signal. Inhibition can act at postsynaptic level (a) or at presynaptic level (b). In each one of the cases inhibition can be the result of a feedforward (c) or a feedback (d) input.

4.4 Possible function of inhibitory circuitry

It is known that the presence of a large GABAergic system in the occipital cortex of mammals is related to contrast or velocity discrimination tasks. In fact, the administration of GABA antagonists impairs the ability to recognize the direction of visual stimuli (Sillito,1977), that is the receptive fields of these neurons are shaped by GABAergic synapses as well as by the spatial arrangement of the dendrites upon which sensory inputs terminate. In lower vertebrate OT, since the ability to discriminate velocity is possessed by retinal ganglion cells, such kind of interpretation seems quite unlikely.
As far as the function of inhibitory GABAergic transmission in the mammalian SC is concerned, experiments have shown that GABA antagonists such as bicuculline or picrotoxin (Dean et al.,1989) induce activation of defence-like reactions, suggesting that a removal or a partial inactivation of the GABA system in the SC "switches" the tectal responses from an orientation to an avoidance response. Such kind of experiments have not so far been performed on *in vivo* amphibians. The complexity of the SC/OT circuitry leads to believe that the inhibitory systems may have several different functions, ranging from processing of visual signal to motor performance. The finding that electrical activity is recorded in the mammalian SC just before a spontaneous saccade in the dark (Glimcher and Spark,1993) indicates that the SC is the source for saccades, and not only the convergence of the visual input before a saccade initiation. This does not look like an exclusive feature of mammalian SC but it could also be present in the lower vertebrates OT (class T5 neurons, Ewert, 1984).
These consideration may be useful to interpret the functional significance of synaptic fatigue upon repeated stimulation as observed in the present study. In fact one might suppose that sustained retinal activity due to stimulation coming from a not point-like source would trigger several simultaneous saccades, a phenomenon which must be prevented to obtain a correct control over visual function. As indicated by the results of our current investigation, the presence of a strong inhibition initiated as soon as activation of tectal neurons is achieved and the threshold for a first saccade is reached, could ensure adequate filtering of the sensory information with a "winner-take-all" strategy for the achievement of the movement and prevention of meaningless "multiple saccades".

References

Antal,M. Distribution of GABA immunoreactivity in the optic tectum of the frog: a light and electron microscopy study. Neuroscience 42: 879-891, 1991.

Arbib,M.A. Modelling neural mechanisms of visuomotor coordination in frog and toad. In Lecture Notes in Biomathematics vol. 45 edited by S. Amari and M.A. Arbib. Heidelberg: Springer-Verlag, 1982, p.342-370.

Bosch,T.J. and Paul,D.H. Differential responses of single reticulospinal cells to spatially localized stimulation of the optic tectum in a teleost fish, Salmo Trutta. Eur. J. Neurosc., 5:742-750, 1993.

Chung,S.H., Bliss,T.V.P. and Keating,M.J. The synaptic organization of optic afferents in the amphibian tectum. Proc. R. Soc. London B.,187: 421-447, 1974.

Colquhoun,D. Lectures on Biostatistics, Oxford: Clarendon press, 1971, p.160-170.

Deisz,R.A. Frequency-dependent depression of inhibition in guinea-pig neocortex *in vitro* by $GABA_B$ receptor feed-back on GABA release. J. Physiol. Lond. 412:513-541, 1989.

Dean,P., Redgrave,P. and Westby,G.W.M. Event or emergency ? Two response system in the mammalian superior colliculus. TINS 12:137-147, 1989.

Dodge,Jr.F.A. and Rahamimoff,R. Co-operative action of calcium ions in transmitter release at the neuromuscular junction. J. Physiol. Lond. 193: 419-432, 1968.

Erulkar,S.D. The modulation of neurotransmitter release at synaptic junctions. Rev. Physiol. Biochem. Pharmacol. 98,63-175, 1983.

Ewert,J.P. in Comparative neurology of the optic tectum, Chapter 11,p.272 ed. Vanegas, Plenum Press, 1984.

Gaze,R.M. The representation of the retina on the optic lobe of the frog. Quart. J. Exp. Physiol. 43:209-226, 1958.

Glimcher,P.W. and Sparks,D.L. Effects of low-frequency stimulation of the superior colliculus on spontaneous and visually guided saccades. J. of Neurophysiol. 69:953-964, 1993.

Hartline,H.K. and Ratliff,F. Inhibitory interaction in the retina of Limulus. In: Handbook of Sensory Physiology, edited by M.G.F. Fuortes. Berlin-Heidelberg: Springer-Verlag, 1972,p.381-447.

Hepp,K.,Van Opstal,A.J., Straumann,D.,Hess,B.J. and Henn,V. Monkey superior colliculus represents rapid eye movements in a two-dimensional motor map. J. of Neurophysiol. 69:965-979, 1993.

Hubbard,J.I., Llinàs,R. and Quastel,M.J., Electrophysiological analysis of synaptic transmission, London: E. Arnold, 1969, p. 267 .

Ikeda,S.R. Double-pulse calcium channel current facilitation in adult rat sympathetic neurones. J. Physiol. Lond. 439:181-214, 1991.

Jacobson,M. The representation of the retina on the optic tectum of the frog. Correlation between the retino-tectal magnification factor and retinal ganglion cell count. J. Exp. Physiol. 47:170-189, 1962.

Kandel,E.R.,Schwartz,J.H. and Jessel,T.M. ,Principles of Neural Sciences, New York, Elsevier, 1991.

Katz,B and Miledi,R. The role of calcium in neuromuscular facilitation. J. Physiol. Lond. 195: 481-492, 1968.

Kobayashi,S., Kishida,R., Goris,R.C., Yoshimoto,M. and Ito,H. Visual and infrared input to the same dendrite in the optic tectum of the Python Regius: electron microscopy evidence. Br. Res. 597:350-352, 1992.

Lazar,G. in Comparative neurology of the Optic Tectum, ed. by Vanegas,H. New York, Plenum press, 1984.

Llinàs,R., Steinberg,I.Z. and Walton,K. Relationship between presynaptic calcium current and postsynaptic potential in squid giant synapse. Biophys. J. 33: 323-352, 1981.

Magleby,K.L. Short term changes in synaptic activity in Synaptic Function. In Synaptic function edited by G.M. Edelman, W.E. Gall and W.M. Cowan. New York: Wiley & Sons Inc., 1987, p.21-56.

Manteuffel,G. and Roth G. A model of the saccadic sensorimotor system of salamanders. Biol. Cyber. 68: 431-440, 1993.

Maturana,H.R., Lettvin,J.Y., McCulloch,W.S. and Pitts,W.H. Anatomy and physiology of the vision in the frog. J. gen. Physiol. 43: 129-170 suppl., 1960.

McDonald,J.W., Cline,H.T., Constantine-Paton,M., Marago,W.F., Johnston,M.V. and Young,A.B. Quantitative autoradiographic localization of NMDA, quisqualate and PCP receptors in the frog optic tectum. Brain Res. 482:155-158, 1989.

Mkrtycheva,L.I. Elements of the functional organization of the visual system in the frog. J. Higher Nerv. Act. P. Pavlov 15:513-524, 1964.

Munoz,P.D. and Wurtz,R.H. Role of the rostral superior colliculus in active visual fixation and execution of the express saccades. J Neurophysiol. 67:1000-1002, 1992.

Nistri,A., Sivilotti,L. and Welsh,D.M. (1990) An electrophysiologic study of the action of N-Methyl-D-Aspartate on excitatory synaptic transmission in the optic tectum of the frog in vitro. Neuropharmacol. 29:681-687, 1990.

Sargent,P.B., Pike,S.H., Nadel,D.B. and Lindstrom,J.M. Nicotinic acetylcholine receptor-like in the retina, retinotectal pathway, and optic tectum of the frog. J. Neurosc. 9(2):565-573, 1989.

Sillito,A.M. Inhibitory processesunderlying the directional specificity of simple, complex and hypercomplex cells in the cat's visual cortex, J. Physiol. Lond. 271:699-720, 1977.
Sivilotti,L. and Nistri,A. An intracellular study of the effects of GABA on frog tectal neurones in vitro. Neurosc. Lett. 154:28-32, 1992.

Sivilotti,L. and Nistri,A. Complex effect of baclofen on synaptic transmission of the frog optic tectum in vitro. Neurosc. Lett. 85:249-254, 1988.

Sivilotti,L. and Nistri,A. Antagonism of the action of glutamate by pentobarbitone or midazolam in the frog optic tectum in vitro. Neuropharmacol. 28:1107-1112, 1989.

Sivilotti,L. and Nistri,A. GABA receptor mechanisms in the central nervous system. Progr. in Neurobiology. 36:35-92, 1991.